Acknowledgement

This work was supported by the Division of Basic Energy Sciences, US Department of Energy. Thanks are extended to Joseph A. Pask for critically viewing the note and to Scott Hewett for conducting some of the experiments.

References

1. B. JAFFE, R. S. ROTH and S. MARZULLO, *J. Res. Natl. Bur. Stand.* 55 (1955) 239.
2. D. A. BERLINCOURT, C. CMOLICK and B. JAFFE, *Proc. Inst. Radio Eng.* 48 (1960) 220.
3. T. IKEDA, Y. TANAKA, T. AYAKAWA and H. NOAKE, *Jap. J. Appl. Phys.* 3 (1964) 581.
4. R. GERSON and H. JAFFE, *J. Phys. Chem. Sol.* 24 (1963) 979.
5. J. J. DIH and R. M. FULRATH, *J. Amer. Ceram. Soc.* 61 (1978) 448.
6. J. F. DULLEA, Jr, M.Sc. thesis, University of California, Berkeley, 1976.
7. K. OKAZAKI and H. IGARASHI, in "Ceramic Monostructure '76" edited by R. M. Fulrath and J. A. Pask (Westview Press, Colorado, 1976) p. 564.
8. D. R. BISWAS, *J. Amer. Ceram. Soc.* 61 (1978) 461.
9. K. OKAZAKI and K. NAGATA, *Trans. Inst. Elect. Commun. Jap.* 53 (1970) 815.
10. R. L. HOLMAN, Ph.D. thesis, University of California, Berkeley, 1972.
11. R. L. HOLMAN and R. M. FULRATH, *J. Appl. Phys.* 44 (1973) 5227.

Received 17 February
and accepted 26 March 1981

J. J. DIH*
D. R. BISWAS†
R. M. FULRATH‡
Materials and Molecular Research Division,
Lawrence Berkeley Laboratory
and Department of Materials Science
and Mineral Engineering,
University of California,
Berkeley,
California 94720,
USA

---

*Present address: Beckman Instruments Inc., Irvine, California 92713, USA.
†Present address: International Telephone and Telegraph Corporation, Roanoke, VA 24019, USA.
‡Deceased July, 1977.

An EXAFS study of amorphous selenium

As part of our programme of study of amorphous chalcogenides we have investigated the extended X-ray absorption fine structure (EXAFS) of glassy selenium. X-ray diffraction studies of amorphous Se have already indicated peaks in the radial distribution function (RDF) at 2.34, 3.78 and 4.97 Å [1]. Structural models suggested for glassy Se indicate that it contains both chains and rings of varying lengths [2]. EXAFS is known to be particularly effective in the study of local structure in glasses [3]. Considering the diverse opinions on the structure of amorphous Se, we felt that an EXAFS study would be instructive.

Se glass was prepared from the 5N purity element (Koch-Light, UK). The K-edge absorption spectrum was recorded on a bent-crystal spectrograph using Mo radiation [4]. A Carl-Zeiss microdensitometer was used to record the trace with a linear reverse dispersion of 0.7 eV mm^{-1}.

Data up to 350 eV beyond the edge were amenable to analysis. Computation of the radial structure function was carried out using a Hanning window function and Eccles' procedure [5]. After background subtraction, the following steps were carried out:

(a) Data between 30 and 350 eV from the edge were Fourier transformed.
(b) The first few components were set equal to zero and data were back-transformed to *k*-space.
(c) Finally a transform to R-space was carried out to yield the radial structure function shown in Fig. 1.

Changes in the integration limits did not shift the positions of the peaks shown in Fig. 1, so that we feel sure that these do represent physical distances and are not computational artefacts. Uncertainties (± 0.02 Å) in the peak positions make estimation of phase-shifts difficult. Nevertheless, the fact that our values for various distances agree quite well with reported values indicates that these shifts are quite small.

In Fig. 1, the peak at 2.34 Å represents the usual Se–Se distance [1]. Apart from the peaks at

0022–2461/81/113222–4$02.40/0

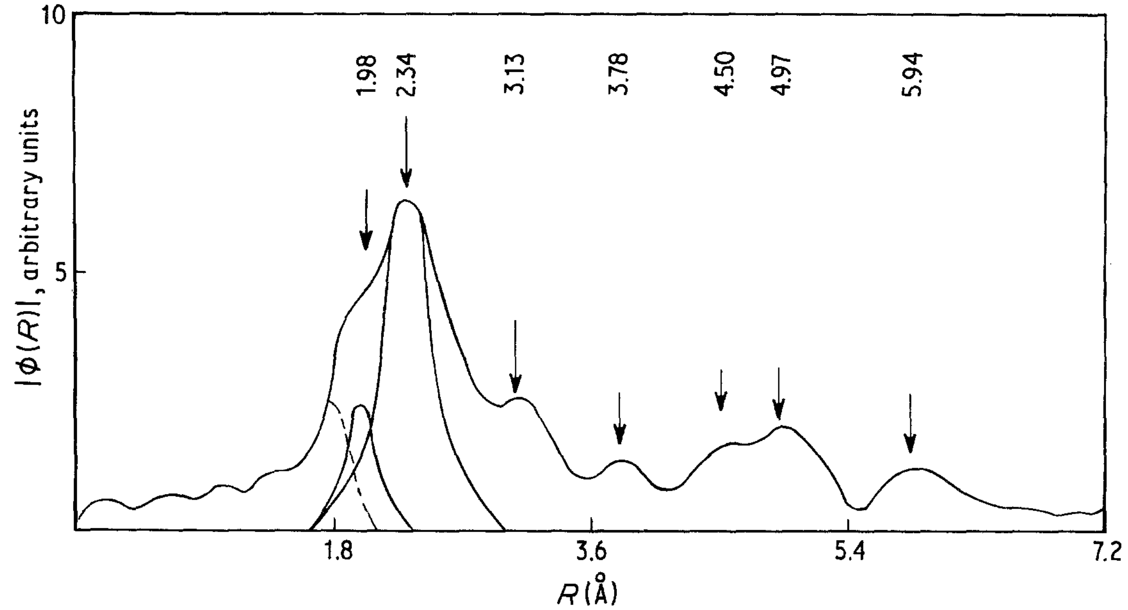

Figure 1 Radial distribution curve for glassy selenium. Distances shown are accurate to ± 0.02 Å.

the distances mentioned earlier, we see additional peaks at 1.98, 3.13, 4.50 and 5.94 Å. As indicated in Fig. 1, the peak at 1.98 Å was obtained through visual deconvolution. While we consider this peak to be the most important, in respect of the distance it represents, its actual area is subject to much uncertainty.

We suggest that the peak at 1.98 Å corresponds to Se–Se double bonds, likely to be present as chain-end Se bonds. Based on this we are able to explain the other three peaks at 3.13, 4.50 and 5.74 Å (Fig. 2). We see that the π-bonds result from an alternate scheme of charged defect formation:

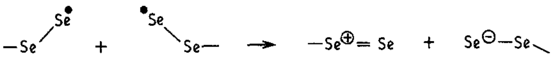

$$-\mathrm{Se}-\overset{\bullet}{\mathrm{Se}} + {}^{\bullet}\mathrm{Se}-\mathrm{Se}- \longrightarrow -\mathrm{Se}^{\oplus}{=}\mathrm{Se} + \mathrm{Se}^{\ominus}-\mathrm{Se}-$$

(1)

Westbury and Cooper [2] have summarized many other studies which indicate the presence of

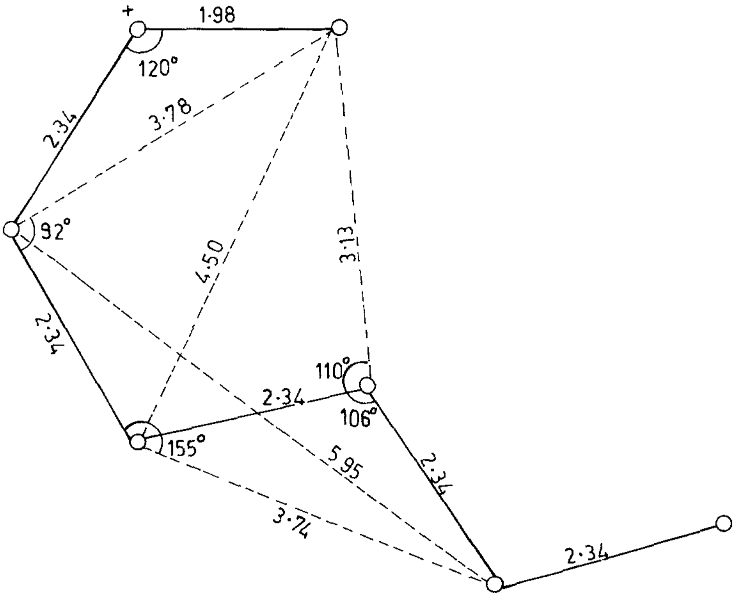

Figure 2 Model of a terminal configuration containing double-bonded selenium.

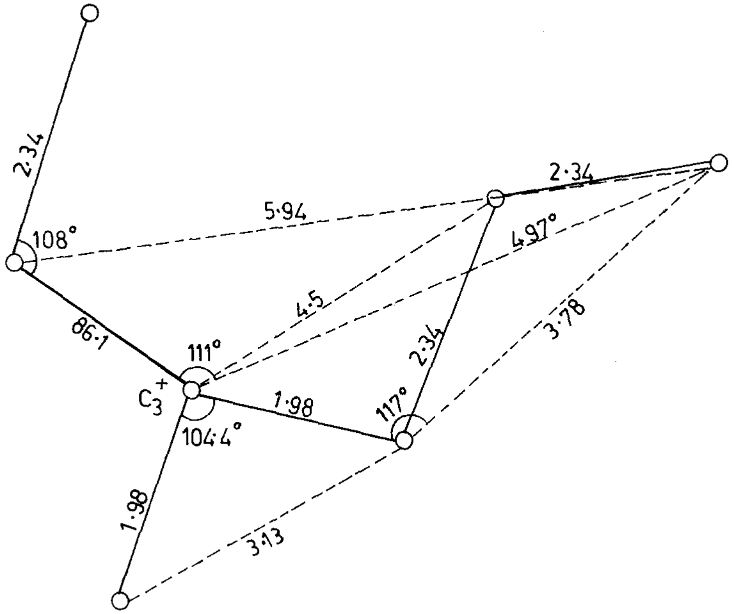

Figure 3 Model of a defect centre containing a C_3^+ defect.

a large number of terminal Se atoms. While there appears to be a wide range of chain-length estimates, it is significant that values as high as 10% can be derived for the fraction of terminal Se atoms on the basis of these studies. More recently, Malaurent and Dixmier [6] had to use a model containing random chains at least 200 atoms long, in order to account for the occurrence of a peak at 5.70 Å in amorphous Se. The fraction of terminal atoms in this case should be at least as high as 1%.

Using the ratio of peak areas in Fig. 1, we estimate that the fraction of terminal Se atoms could be 7 ± 3%. However, we emphasize that quantitative estimates based on EXAFS are, in general, error prone. The transform ripple present in the radial structure function, for example, vitiates such estimates. The comparatively high concentration of terminal Se atoms that we see could possibly be caused by extended irradiation.

The infra-red spectrum of amorphous Se reported by Lucovsky [7] shows a shoulder at 230 cm^{-1} which has been attributed to a fundamental vibration. Since the frequency of this vibration is roughly 1.6 times the Se–Se stretching frequency, we wonder whether it can be attributed to Se=Se double bonds of the nature described above.

It is interesting to speculate on an alternative explanation for the 1.98 Å distance in glassy Se. Kastner *et al.* [8] have suggested the existence of C_3^+-type defect centres. Such centres would be expected to have short bond lengths since charged defects are stabilized only when the overlap integral is large. Enhanced overlap requires the formation of short bonds, the shortness in this case being accentuated by the presence of a positive charge. One can visualize a model based on C_3^+ centres which also accounts for all the distances, as shown in Fig. 3.

The explanation based on C_3^+ centres is however, not entirely satisfactory since the concentration of such defects should be extremely small.

Acknowledgements

We are grateful to Professor C. N. R. Rao for very helpful discussions and critical reading of the manuscript. Dr. M. K. Uppal was of much help in rendering the EXAFS program operational.

References

1. R. KAPLOW, T. A. ROWE and B. L. AVERBACH, *Phys. Rev.* 168 (1968) 1068.
2. R. A. WESTBURY and W. C. COOPER, in "Selenium", edited by R. A. Zingaro and W. C. Cooper (Van Nostrand Reinhold Company, New York, 1979).
3. J. WONG and C. A. ANGELL, "Glass: Structure by Spectroscopy" (Marcel Decker, New York, 1976).
4. P. R. SARODE, K. J. RAO, M. S. HEGDE and C. N. R. RAO, *J. Phys. C: Sol. Stat. Phys.* 12 (1979) 4119.
5. T. K. ECCLES, Stanford Synchrotron Research

Laboratory Report 78/01, Stanford University, Stanford, CA 94305, USA.
6. J. C. MALAURENT and J. DIXMIER, in "The Structure of Non-Crystalline Materials", edited by P. H. Gaskell (Taylor and Francis, London, 1977) p. 49.
7. G. LUCOVSKY, *Mater. Res. Bull.* 4 (1969) 505.
8. M. KASTNER, D. ADLER and H. FRITZCHE, *Phys. Rev. Letts.* 37 (1976) 1067.

Received 17 February
and accepted 25 March 1981

R. PARTHASARATHY
P. R. SARODE
K. J. RAO
Solid State and Structural Chemistry Unit,
Indian Institute of Science,
Bangalore-560012,
India

Debye temperatures of oxides with the NaCl structure

The characteristic Debye temperature is an important parameter which features in descriptions of the thermal and elastic properties of a solid. Traditionally, Debye temperatures (calorimetric, θ_{cal}) are obtained from heat capacity measurements, but values may also be calculated from elastic constants (θ_{el}). A number of high precision techniques for the latter procedure have been reviewed by Alers [1], and Konti and Varshni [2]. At temperatures close to absolute zero θ_{cal} is usually very close to θ_{el}.

Debye temperatures have been published for a wide variety of solids [1–4], but despite their relative simplicity, there are only limited data for oxides having the NaCl structure. Elastic constants of varying reliability are now available for most of these oxides and thus θ may be readily calculated.

By considering only acoustic branches of the phonon dispersion spectrum of a diatomic solid, the elastic Debye temperature at 0 K may be approximated to

$$\theta_{\text{el}} = \frac{h}{k}\left(\frac{3pN\rho}{4\pi M}\right)^{1/3} \cdot V_{\text{m}}, \qquad (1)$$

where h is Planck's constant, k is Boltzmann's constant, p is the number of atoms in the molecule (i.e. 2 in this case), N is Avogadro's number, ρ is density, M is molecular weight and V_{m} is the mean sound velocity defined by

$$V_{\text{m}} = \left(\frac{1}{3}\sum_{i=1}^{3}\int_V \frac{1}{V_i^3}\frac{\mathrm{d}\Omega}{4\pi}\right)^{-1/3}, \qquad (2)$$

i.e. the average of all the direction-dependent velocities V_i [3]. When the individual elastic moduli are available, the integral in Equation 2 may be solved by using one of the high precision techniques [1, 2].

Alternatively, for isotropic crystals, an approximate value may be obtained from

$$V_{\text{m}} = \left[\frac{1}{3}\left(\frac{2}{V_{\text{s}}^3}+\frac{1}{V_{\text{p}}^3}\right)\right]^{-1/3}, \qquad (3)$$

where V_{s} and V_{p} are the transverse sound velocity and longitudinal sound velocity, respectively [3].

TABLE I Elastic moduli, densities and calculated Debye temperatures of some NaCl structure oxides

Oxide	Elastic moduli ($\times 10^{10}$ Nm^{-2})			Density ($\times 10^3$ kg m^{-3})	Reference	$\theta_{\text{(calc)}}$ (K)
	C_{11}	C_{12}	C_{44}			
BaO	12.440	4.869	3.368	5.992	[5]	292.3
SrO	17.354	4.715	5.587	5.009	[5]	441.4
CoO	25.911	14.87	8.268	6.438	[6]	517.8
MnO	22.3	12.0	7.90	5.39	[7]	525.7
CaO	22.063	5.655	8.032	3.346	[5]	673.6
MgO	29.404	9.248	15.581	3.579	[8]	939.1

0022–2461/81/113225–3$02.30/0